Asp338 Controls Hydride Transfer in *Escherichia coli* IMP Dehydrogenase†

Kathleen M. Kerr,‡,§ Jennifer A. Digits,‡,|| Nicolas Kuperwasser,⊥ and Lizbeth Hedstrom*,‡

Departments of Biochemistry and Biology, Brandeis University, Waltham, Massachusetts 02454

Received March 8, 2000; Revised Manuscript Received May 8, 2000

ABSTRACT: IMP dehydrogenase (IMPDH) catalyzes the oxidation of IMP to XMP with the concomitant reduction of NAD^+. This reaction involves the formation of a covalent adduct with an active site Cys. This intermediate, E-XMP*, hydrolyzes to produce XMP. The mutation of Asp338 to Ala severely impairs the activity of *Escherichia coli* IMPDH, decreasing the value of k_{cat} by 650-fold. No ^DV_m or $^DV/K_m$ isotope effects are observed when 2-^{2}H-IMP is the substrate for wild-type IMPDH. Values of $^DV_m = 2.6$ and $^DV/K_m$ (IMP) = 3.4 are observed for Asp338Ala. Moreover, while a burst of NADH production is observed for wild-type IMPDH, no burst is observed for Asp338Ala. These observations indicate that the mutation has decreased the rate of hydride transfer by at least 5×10^3-fold. In contrast, k_{cat} for the hydrolysis of 2-chloroinosine-5′-monophosphate is decreased by only 8-fold. In addition, the rate constant for inactivation by 6-chloropurine riboside 5′-monophosphate is increased by 3-fold. These observations suggest that the mutation has little effect on the nucleophilicity of the active site Cys residue. These results are consistent with a recent crystal structure that shows a hydrogen bonding network between Asp338, the 2′-OH of IMP, and the amide group of NAD^+ [Colby, T. D., Vanderveen, K., Strickler, M. D., Markham, G. D., and Goldstein, B. M. (1999) *Proc. Natl. Acad. Sci. U.S.A.* 96, 3531−3536].

IMPDH[1] catalyzes the oxidation of IMP to XMP with the concomitant reduction of NAD^+ to NADH (Figure 1). This reaction is the rate-limiting step in guanine nucleotide biosynthesis. IMPDH inhibitors have antiproliferative activity and may be useful antiviral, anticancer, antimicrobial, and immunosuppressive agents (*1*−*4*).

The IMPDH reaction is initiated by attack of an active site Cys (Cys305 in *Escherichia coli* numbering) on the 2 position of IMP to form a covalent E-IMP intermediate (Figure 1). A hydride is then transferred to NAD^+ producing NADH and an E-XMP* intermediate (*5*−*7*). E-XMP* subsequently hydrolyzes to release XMP and regenerate the free enzyme, possibly via a second tetrahedral intermediate E-XMP†. Many of the details of the mechanism of Figure 1 have not been substantiated, for example, (i) are nucleophillic addition and hydride transfer stepwise (as shown) or concerted? (ii) How is the putative oxyanion stabilized? (iii) Which tautomer of XMP is released by the enzyme? and (iv) What is the base that activates water?

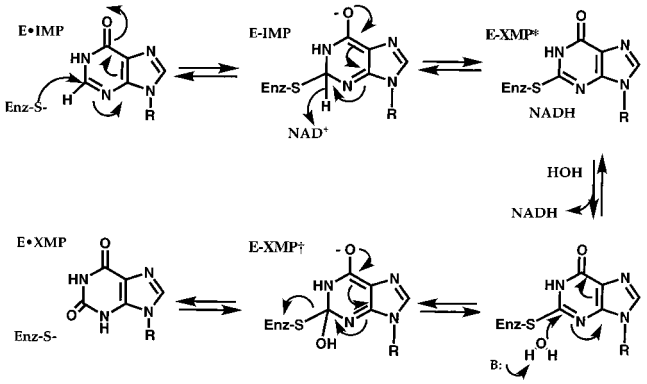

FIGURE 1: Proposed mechanism for the IMPDH reaction.

No obvious candidate for a base to activate water has emerged from the IMPDH crystal structures solved to date. Sintchak et al. have proposed that the side chains of a Thr and Gln residue form a binding pocket that activates water (*7*). Although the Thr residue is conserved, either Gln or Glu are found at the other position (these residues are Thr307 and Glu415 in *E. coli* IMPDH numbering; the corresponding Chinese hamster numbering is shown in Table 1). Moreover, the mutation of this Thr to Ile has little effect on activity (*7*). These observations suggest that these residues are not important components of the catalytic machinery of IMPDH.

† Funded by NIH Molecular Structure and Function Training Grant GM07956 (K.M.K., J.A.D.), NIH Grant GM54403 (L.H.), and a grant from the Lucille P. Markey Charitable Trust to Brandeis University. L.H. is a Searle Scholar and a Beckman Young Investigator.

* To whom correspondence should be addressed: Department of Biochemistry, Brandeis University MS 009, 415 South Street, Waltham, MA 02454; phone: (781) 736-2333; fax: (781) 736-2349; e-mail: hedstrom@brandeis.edu.

‡ Department of Biochemistry.

§ Present address: United States Patent and Trademark Office, Recombinant Enzymology Art Unit, Crystal Mall 1, 1911 South Clark Place, Arlington, VA 22202 (703) 308-0196.

⊥ Department of Biology.

|| Present address: Department of Pharmacology and Cancer Biology, Duke University Medical Center, Levine Science and Research Center, Durham, NC 27710.

[1] Abbreviations: IMPDH, inosine 5′-monophosphate dehydrogenase; IMP, inosine 5′-monophosphate; NAD^+, nicotinamide adenine dinucleotide; NADH, reduced nicotinamide adenine dinucleotide; XMP, xanthosine 5′-monophosphate; GMP, guanosine 5′-monophosphate; MPA, mycophenolic acid; EICARMP, 5-ethynyl-1-β-D-ribofuranosylimidazole-4-carboxamide 5′-monophosphate; 6-Cl-IMP, 6-chloropurine riboside 5′-monophosphate; dIMP, 2-deoxyinosine 5′-monophosphate; DTT, dithiothreitol; 2-Cl-IMP, 2-chloroinosine-5′-monophosphate; SAD, selenazole-4-carboxamide adenine dinucleotide; EDTA, ethylene diaminotetraacetic acid; APAD, acetylpyridine adenine dinucleotide.

10.1021/bi0005409 CCC: $19.00
Published on Web 07/19/2000

Table 1: *E. coli* and Chinese Hamster IMPDH Numbering

E. coli	Chinese hamster
Cys305	Cys331
Thr307	Thr333
Glu415	Gln441

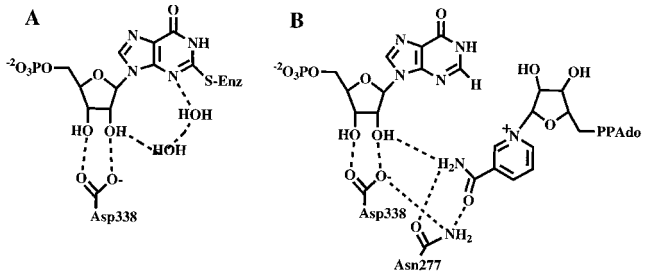

FIGURE 2: Interactions of Asp338. (A) Asp338 in the E-XMP*• mycophenolic acid complex (*7*). (B) Asp338 in the 6-Cl-IMP inactivated enzyme complexed with SAD (*9*).

Zhang et al. have proposed that Tyr450 acts as the general base in IMPDH from *Streptococcus pyogenes* (*8*). However, this Tyr is also not conserved, and mutation of this residue has little effect on activity (this residue is Leu444 in *E. coli* IMPDH). All IMPDH structures contain large regions of disorder that may conceal the catalytic base (*7*−*10*).

A water molecule forms a hydrogen bond to N3 of the purine ring in the E-XMP* and E•IMP complexes (*7*, *8*). This water molecule is linked to Asp338 via a hydrogen bonding network including another water molecule and the 2′-OH of IMP (Figure 2A). This network might provide a means of activating water for hydrolysis of E-XMP*. The substitution of Asp338 with Ala profoundly impairs the activity of *E. coli* IMPDH, decreasing the value of k_{cat} by 600-fold and the value of K_i for GMP and XMP by 5−10-fold (*11*). These observations suggest that Asp338 is not simply involved in IMP binding but is also intimately involved in the chemical transformation. This observation is consistent with the activation of water via a hydrogen bonding network involving Asp338. Alternatively, the recent structure of 6-Cl-IMP inactivated IMPDH complexed with an NAD^+ analogue (SAD) suggests that Asp338 is involved in a hydrogen bonding network linking IMP to the nicotinamide base of NAD^+ (Figure 2B) (*9*). This network would be expected to influence the rate of hydride transfer by orienting the nicotinamide ring relative to the hypoxanthine ring of IMP.

In the present paper, we report the further characterization of Asp338Ala. These results suggest that Asp338 is primarily required for hydride transfer, most likely via a hydrogen bonding network involving the 2′-OH of IMP. The identity of the catalytic base remains unknown.

MATERIALS AND METHODS

Materials. IMP, dIMP, 6-Cl-IMP, and Tris were purchased from Sigma. NAD^+ was purchased from Boehringer Mannheim. DTT was purchased from Research Organics, Inc. Glycerin, EDTA, and KCl were purchased from Fisher. EICARMP was the gift of Dr. Akira Matsuda (Hokkaido University, Japan) and 2-Cl-IMP was the generous gift of Dr. George D. Markham (Fox Chase Cancer Center, Philadelphia, PA). Oligonucleotides were obtained from the Brandeis Oligonucleotide Facility. 2-^{2}H-IMP was synthesized as previously described (*12*).

Methods. Site-directed mutagenesis was performed using Quikchange (Stratagene, La Jolla, CA). Enzymes were expressed under control of the natural promoter in the LH3 cells, which carry a deletion in *guaB* and are recombination-deficient (*11*). Enzyme was purified as previously described (*11*). Preparations were judged >90% homogeneous by SDS−PAGE stained with Coomassie Blue. Enzyme concentration was determined by titration with EICARMP (*13*).

Enzyme Kinetics. Assays were typically performed in 50 mM Tris, pH 8.0, 100 mM KCl, 3 mM EDTA, and 1 mM DTT with appropriate concentrations of IMP and NAD^+ at 25 °C. The production of NADH was monitored either by change in absorbance at 340 nm on a Hitachi U2000 or by changes in fluorescence (excitation wavelength 340 nm, emission wavelength 460 nm) in a PerSeptive Biosystems Cytofluor II multiwell plate reader. The reactions of wild-type IMPDH display strong NAD^+ substrate inhibition. Therefore, the Michaelis−Menten parameters for wild-type IMPDH were determined by fitting initial rate data versus IMP concentrations at fixed NAD concentrations to the Michaelis−Menten equation (eq 1). The V_{max} values derived from these fits were re-plotted versus NAD^+ concentration and fit to an equation describing substrate inhibition (eq 2) to determine k_{cat} and K_m and K_{ii} for NAD^+. To determine the value of K_m for IMP, the initial velocity data versus NAD^+ concentration were fit to eq 2. The apparent values of k_{cat} were re-plotted versus IMP concentration and fit to eq 1. The fits were performed using Kaleidagraph software (Abelbeck Software) (*11*, *14*).

$$v/E = k_{cat}[\mathrm{IMP}]/(K_{\mathrm{IMP}} + [\mathrm{IMP}]) \quad (1)$$

$$v/E = k_{cat}[\mathrm{NAD^+}]/(K_m + [\mathrm{NAD^+}] + [\mathrm{NAD^+}]^2/K_{ii}) \quad (2)$$

where v is the initial velocity, E is the enzyme concentration, k_{cat} is the overall rate constant, A is the concentration of IMP or dIMP, K_a is the Michaelis−Menten constant for IMP or dIMP, K_{NAD} is the Michaelis−Menten constant for NAD^+, and K_{ii} is the substrate inhibition constant for NAD^+.

No NAD^+ substrate inhibition was observed in the reaction of Asp338Ala. Therefore, these data were fit to a sequential mechanism (eq 3) using KinetAsyst software (Intellikinetics):

$$v/\mathrm{E} = k_{cat}A[\mathrm{NAD^+}]/(K_{ia}K_{NAD} + K_a[\mathrm{NAD^+}] + K_{NAD}A + A[\mathrm{NAD^+}]) \quad (3)$$

where K_{ia} is the dissociation constant for IMP or dIMP from the binary E•A complex. Primary deuterium isotope effects were determined by comparing the values of V_m and V_m/K_m for the reactions with IMP and 2-^{2}H-IMP. The hydrolysis of 2-Cl-IMP was monitored by the change in absorbance at 286 nm ($\Delta\epsilon = 6.2 \times 10^3\ \mathrm{M^{-1}\ cm^{-1}}$) as previously described (*15*, *16*).

Pre-steady-state experiments were performed on an Applied Photophysics SX.17MV stopped flow spectrophotometer at 25 °C. The production of NADH was monitored either by fluorescence (excitation wavelength 340 nm, 420 nm cutoff emission filter) or by absorbance at 340 nm. Concentrations indicated in the text or figure legends are the final concentrations after mixing. The time course of fluorescence

or absorbance can be described by a single-exponential equation with a steady-state term (eq 4):

$$S_t = (A)\exp(-k_{obs}t) + vt \quad (4)$$

where S_t is the signal (fluorescence or absorbance) at time t, A is the amplitude of the burst, k_{obs} is the observed first-order rate constant governing the burst phase, and v is the linear rate of increase in fluorescence or absorbance during steady state. The maximum value of k_{obs} for the reaction monitored by absorption is designated k_{burst}. The maximum value of k_{obs} for the reaction monitored by fluorescence is designated k_{fluor}.

Inactivation of IMPDH by EICARMP and 6-Cl-IMP. Asp338Ala (2.8 μM) was incubated with various concentrations of EICARMP (0−75 μM), 750 μM IMP, and 8 mM NAD^+ in assay buffer, and NADH production was monitored over 2 min. The progress curves were fit to eq 5:

$$F - F_o = v_o/k_{obs}[1 - \exp(-k_{obs}t)] \quad (5)$$

where F and F_o are the fluorescence at time t and time 0 respectively, v_o is the initial rate at time = 0, and k_{obs} is the observed rate constant of inactivation. Less than 10% of the substrates were consumed in all assays. The values of k_{obs} displayed a linear dependence on EICARMP concentration, as observed previously with wild-type IMPDH (*13*), and were fit to eq 6:

$$k_{obs} = k_{on}I/(1 + A/K_a) \quad (6)$$

where k_{on} is the apparent second-order rate constant for the reaction of EICARMP and IMPDH.

Wild-type and Asp338Ala IMPDH were incubated with 6-Cl-IMP in 5−100-fold molar excess in 50 mM Tris, pH 7.5, and 10% glycerol at 25 °C for up to 5 min. Aliquots were removed at appropriate time intervals and quenched by dilution into assay buffer without DTT. Remaining enzyme activity was measured at 1 mM IMP and 2.5 mM NAD^+ (wild-type) or 8 mM IMP and 8 mM NAD^+ (Asp338Ala). The inactivation of both wild-type and Asp338Ala followed pseudo-first-order kinetics. The data were fit to eq 7:

$$\ln(v_t/v_0) = -k_{obs}t \quad (7)$$

where v_t is the activity at time t and v_0 is the activity at time = 0. The values of k_{obs} displayed a hyperbolic dependence on 6-Cl-IMP concentration, which suggests that inactivation follows a two-step mechanism where E·I is a reversible complex and EI* is the irreversibly inactivated enzyme:

$$E + I \underset{k_1}{\overset{k_{-1}}{\rightleftharpoons}} E\cdot I \xrightarrow{k_{inact}} EI^* \quad (8)$$

This mechanism of inactivation has been previously observed in the 6-Cl-IMP inactivation of *E. coli* and human type 2 IMPDHs as well as in the inactivation of GMP reductase (*16*−*18*). The values of k_{obs} were fit to eq 9:

$$k_{obs} = k_{inact}[I]/([I] + K_i) \quad (9)$$

where I is the concentration of 6-Cl-IMP and K_i is the apparent dissociation constant of 6-Cl-IMP.

Table 2: Steady-State Kinetic Parameters for Wild-Type and Asp338Ala IMPDH[a]

	wild-type		Asp338Ala	
	IMP	dIMP	IMP	dIMP
k_{cat}, s^{-1}	13 ± 1[b]	4.4 ± 0.7	0.02 ± 0.01[b]	0.003 ± 0.001
K_m substrate, μM	60 ± 9[b]	110 ± 10	700 ± 100[b]	2600 ± 1000
K_m NAD^+, mM	2.0 ± 0.5[b]	3.9 ± 0.9	3.3 ± 0.4[b]	5.8 ± 2
K_{ii} NAD^+, mM	2.8 ± 0.8[b]	7.9 ± 2.5	na	na
K_i XMP, μM	130 ± 20[b]	nd	600 ± 120	nd
K_i GMP, μM	90 ± 20[b]	nd	510 ± 80	nd
k_{cat}/K_mK_m, $s^{-1}M^{-2}$	11 × 10^7	1 × 10^7	8600	900
$^DV_{max}$	1.2 ± 0.3	nd	2.6 ± 0.3	nd
$^DV/K_m$(IMP)	1.0 ± 0.5	nd	3.4 ± 1.6	nd
$^DV/K_m$(NAD^+)	1.6 ± 0.8	nd	1.3 ± 0.5	nd

[a] Conditions as described in Materials and Methods; na, not applicable (no NAD^+ substrate inhibition is observed); nd, no data. [b] Values from ref *11*.

RESULTS

Kinetic Isotope Effects on the Reactions of Wild-Type and Asp338Ala IMPDHs. A summary of the Michaelis−Menten parameters of wild-type and Asp338Ala IMPDHs are shown in Table 2 (*11*). Wild-type IMPDH is strongly inhibited by high concentrations of NAD^+. This NAD^+ substrate inhibition is more pronounced than that observed in IMPDHs from other sources (*12*, *17*, *18*). This inhibition is uncompetitive with respect to IMP and is believed to result from formation of an E-XMP*·NAD^+ complex (*18*, *19*). Unfortunately, this NAD^+ substrate inhibition introduces considerable error into the determination of V_{max} and the associated isotope effects. Nevertheless, it is apparent that no isotope effect is observed on V_{max} when 2-^{2}H-IMP is the substrate. This observation indicates that hydride transfer is not rate-limiting. The absence of a V_{max} isotope effect has also been reported for human type 2 and *Tritrichomonas foetus* IMPDH (*12*, *18*, *20*). In addition, no isotope effects are observed on V_{max}/K_m for either IMP or NAD^+ when 2-^{2}H-IMP is the substrate. This observation suggests that both IMP and NAD^+ are "sticky" substrates (*21*) and is consistent with a random mechanism as observed in human type 2 and *T. foetus* IMPDHs.

As reported previously, the value of k_{cat} is decreased by 650-fold in the Asp338Ala mutant, while only modest changes in the values of K_m for IMP and K_i for IMP analogues are observed (Table 2) (*11*). No NAD^+ inhibition is observed in the reaction of Asp338Ala. These observations suggest that the mutation of Asp338 primarily impairs the chemical transformation steps rather than substrate binding. In contrast to wild-type IMPDH, a V_{max} isotope effect of 2.6 is observed when 2-^{2}H-IMP is the substrate (Table 1). This observation indicates that hydride transfer is at least partially rate-limiting for Asp338Ala and suggests that the rate of hydride transfer must have been decreased by at least a factor of 3300 (in wild type, hydride transfer is not rate-limiting and must therefore be $\geq 5 \times k_{cat}$; since k_{cat} is reduced by 650× in the mutant, hydride transfer must be reduced by ≥3300). In addition, no V_{max}/K_m isotope effect is observed for NAD^+, but a significant V_{max}/K_m isotope effect is observed for IMP. These observations indicate that NAD^+

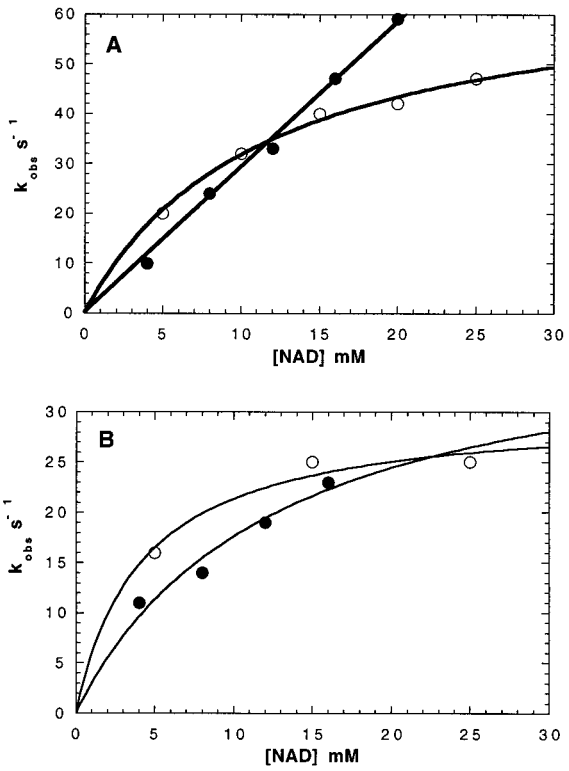

FIGURE 3: Dependence of the burst phase on NAD^+ concentration for the wild-type IMPDH reaction. Values of k_{obs} are plotted against NAD^+ concentration. Reaction conditions: 50 mM Tris, pH 8.0, 100 mM KCl, 3 mM EDTA and 1 mM DTT. Enzyme (1−5 μM) was preincubated with IMP (2 mM) or dIMP (10 mM) and mixed with an equal volume of buffer containing NAD^+. The final concentration of NAD^+ is listed on the graph. Progress curves were fit to eq 4 as described previously (*18*, *24*, *30*). (A) IMP reaction. Values of k_{obs} for the reaction monitored by absorption at 340 nm are denoted by the closed circles. Values of k_{obs} for the reaction monitored by fluorescence (excitation 340 nm, emission 420 nm cutoff filter) are denoted by the open circles. (B) dIMP reaction. Values of k_{obs} for the reaction monitored by absorption at 340 nm are denoted by the closed circles. Values of k_{obs} for the reaction monitored by fluorescence are denoted by the open circles.

remains a sticky substrate, while IMP can dissociate from the E·IMP·NAD^+ complex. This result indicates that the mutation of Asp338 perturbs IMP binding in addition to decreasing the rate of hydride transfer. Further, these results suggest that Asp338Ala operates via an ordered kinetic mechanism whereby NAD^+ binds first followed by IMP (*21*). This mechanism contrasts with the apparently random mechanism of wild-type *E. coli* IMPDH as well as the "IMP first" ordered mechanisms initially proposed for many IMPDHs (*17*, *22*, *23*).

Pre-Steady-State Kinetics. A burst of NADH production is observed when wild-type E·IMP is mixed with NAD^+ and the reaction is monitored by absorbance at 340 nm. The data fit to a single-exponential equation with a steady-state term (eq 4) (*24*). This observation confirms that hydride transfer is not rate-limiting. The rate constants for the exponential phase (k_{obs}) display a linear dependence on NAD^+ concentration (Figure 3), which suggests that NAD^+ binds to E·IMP with a $K_{app} \geq 70$ mM and that the maximum value, k_{burst}, must be ≥ 200 s^{-1} (these limits are derived as follows: significant deviation from linearity will be observed when $[NAD^+]$ is $0.3 \times K_{app}$; therefore, since a linear dependence is observed to 20 mM NAD, then $K_{app} \geq 20/0.3 = 70$ mM. The slope of this line is equivalent to k_{burst}/K_{app}; therefore, $k_{burst} \geq 200$ s^{-1}). The amplitude of the burst phase is 0.5 NADH/active site. A similar burst has been observed in the reaction catalyzed by IMPDH from *T. foetus* (*18*).

A burst is also observed when the reaction is monitored by NADH fluorescence. The data were also fit to a single exponential with a steady-state term (eq 4). However, the values of k_{obs} displayed a hyperbolic dependence on NAD^+. The maximum value, k_{fluor}, is smaller than k_{burst} (Figure 3). These observations suggest that absorbance and fluorescence monitor different steps in the IMPDH reaction. We believe that the fluorescence of enzyme-bound NADH is initially quenched. Purines such as E-XMP* are known quenchers. The reduced nicotinamide ring should be close to the purine ring of E-XMP* and would therefore be quenched. Fluorescence is observed when the environment of reduced nicotinamide ring subsequently changes, either by dissociation of NADH or by a conformational change. Similar behavior was observed for IMPDH from *T. foetus*, where k_{fluor} was assigned to NADH release (*18*). Therefore, we have assigned the $k_{fluor} = 40$ s^{-1} to the dissociation of NADH. Since the dissociation of NADH is slow relative to the hydride transfer step, the E·IMP·NAD^+ and E-XMP*·NADH complexes will be at equilibrium. Under our experimental conditions, the E·IMP complex is preformed and the reaction is initiated with NAD^+ in the presence of saturating IMP. Therefore, E·IMP·NAD^+ is the only NAD^+ complex. Our previous work with IMPDH from other sources indicates that NADH release precedes hydrolysis of E-XMP* (*12*, *18*). Assuming the same mechanism applies to the *E. coli* enzyme, then the only NADH complex is E-XMP*·NADH. Therefore, the amplitude of 0.5 NADH/active site indicates that K_{eq} for the hydride transfer step (i.e., the interconversion of E·IMP·NAD^+ and E-XMP*·NADH) is 1. Similar observations have been made in *T. foetus* IMPDH (*18*). Two other explanations for the amplitude of 0.5 should be considered: (i) only half of the active sites are operative or (ii) the absorbance spectrum of NADH is altered in the E-dXMP*·NADH. We have shown that the amplitude increases to 0.8 when NAD^+ is replaced with APAD in *T. foetus* IMPDH (*18*). This observation argues strongly against half-sites activity. Unfortunately, we cannot measure the absorption coefficient of NADH in the E-dXMP*·NADH complex. However, we note that if the absorption coefficient of NADH was different when bound to the enzyme, then a second exponential phase would be observed corresponding to the release of NADH. We see no evidence for such a phase, which suggests that the absorbance spectra of free and bound NADH are similar.

No burst of NADH production is observed in the reaction of Asp338Ala with IMP, which confirms that hydride transfer is rate-limiting for this mutant. This result indicates that the mutation of Asp338 decreases the rate of hydride transfer by at least 5×10^3-fold.

Reaction of Wild-Type and Asp338Ala IMPDHs with dIMP. The reaction of IMPDH with dIMP was investigated to probe the interaction between Asp338 and the 2′-OH group of IMP. The values of k_{cat}, K_m, and K_{ii} for NAD^+ are similar to those of the IMP reaction (within 2−3-fold; Table 2). Similar results have been reported for Sarcoma 180 cell and human type 2 IMPDHs (*16*, *25*). The reaction of dIMP with Asp338Ala is also similar to the IMP reaction. The values of k_{cat} and K_m are within 2−3-fold of those of the IMP

Table 3: Pre-Steady-State Kinetic Rate Constants[a]

beg complex	k_{burst} (s^{-1})	K_{app} (mM)	amplitude (NADH/enzyme)	k_{fluor} (s^{-1})	$K_{app,fluor}$ (mM)
E·IMP	≥ 200[b]	≥ 70[b]	0.56 ± 0.08	44 ± 3	4 ± 1
E·dIMP	43 ± 12	15 ± 7	0.54 ± 0.02	38 ± 8	6 ± 4

[a] Conditions are as described in Figure 3. [b] Estimated from the data of Figure 3, assuming that $K_{app} \geq 3.3 \times 20$ mM.

reaction (Table 2). These results would seem to suggest that the interaction between Asp338 and the 2′-OH of IMP is of little consequence.

However, the pre-steady state kinetics of the dIMP reaction are significantly different from those of IMP. A burst of NADH production is observed when E·dIMP is mixed with NAD^+. The amplitude of the burst phase is 0.5 NADH/active site as measured by absorbance. A hyperbolic dependence of k_{burst} on NAD^+ concentration is observed, with $K_{app} = 6$ mM (Table 3). The maximum value of $k_{burst} = 40\ s^{-1}$ and has been assigned to hydride transfer. This result indicates that the loss of the 2′-OH group of IMP decreases the rate of hydride transfer by at least 5-fold. Unlike the IMP reaction, the value of k_{obs} is similar to that of k_{fluor} (Figure 3). This observation suggests that absorbance and fluorescence monitor the same step in the dIMP reaction. This conclusion implies that either: (i) the dissociation of NADH from E-dXMP*·NADH is fast relative to hydride transfer or (ii) enzyme-bound NADH is not quenched in complex with E-dXMP*. In the first case, an equilibrium will not be established and the amplitude of the burst phase will be 1 NADH/active site. Therefore, we believe that the fluorescence of NADH is not quenched in the E-dXMP*·NADH complex. It is possible that quenching requires the presence of the hydrogen bond between the 2′-hydroxyl of IMP and the amide nitrogen of reduced nicotinamide. This bond orients the nicotinamide and purine rings; in its absence the E-dXMP* and the reduced nicotinamide ring may no longer be held in close proximity, and fluorescence may not be quenched.

Inactivation of Wild-Type and Asp338Ala IMPDH. Both EICARMP and 6-Cl-IMP inactivate IMPDH by alkylating the active site Cys (Figure 4panels A and B) (*13*, *26*, *27*). Therefore, these reactions can be used to probe the effect of Asp338 → Ala mutation on the reactivity of the active site Cys. The inactivation of Asp338Ala by EICARMP was monitored by progress curve analysis (eq 5) (Figure 5A). Although EICARMP most likely inactivates IMPDH via a two-step mechanism as in eq 8, the values of k_{obs} for inactivation of both wild-type and Asp338Ala enzymes are linearly dependent on EICARMP concentration (Figure 5B) (*13*). This observation suggests that the value of K_i must be in excess of 40 μM (k_{obs} is a linear function of [EICARMP] to 80 μM, which suggests that K_i is in excess of 80 μM; however, since EICARMP and IMP compete for the same site, this limit must be revised downward by a factor of $(1 + [IMP]/K_m) = \sim 2$, so $K_i \gg 40$ μM). Unfortunately, the reaction is too rapid to be monitored at higher concentrations of EICARMP. Therefore, values of K_i and k_{inact} cannot be obtained, and we are unable to determine the effect of the mutation on the alkylation step independent of EICARMP binding. The value of k_{on} is decreased 60-fold from that of wild-type IMPDH (Table 4). Assuming that the binding of

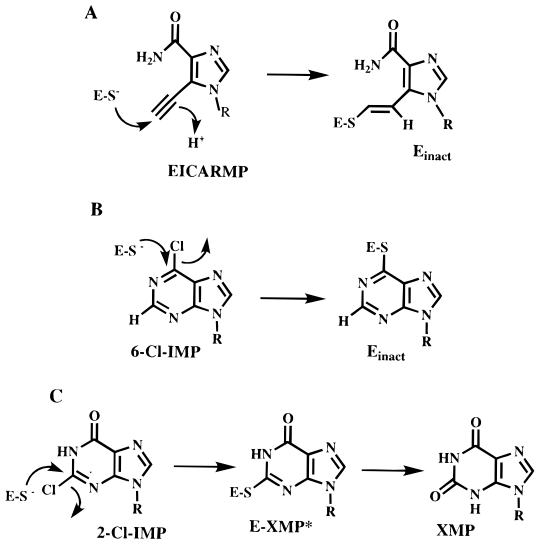

FIGURE 4: Reactions of IMPDH. (A) EICARMP; (B) 6-Cl-IMP; (C) 2-Cl-IMP.

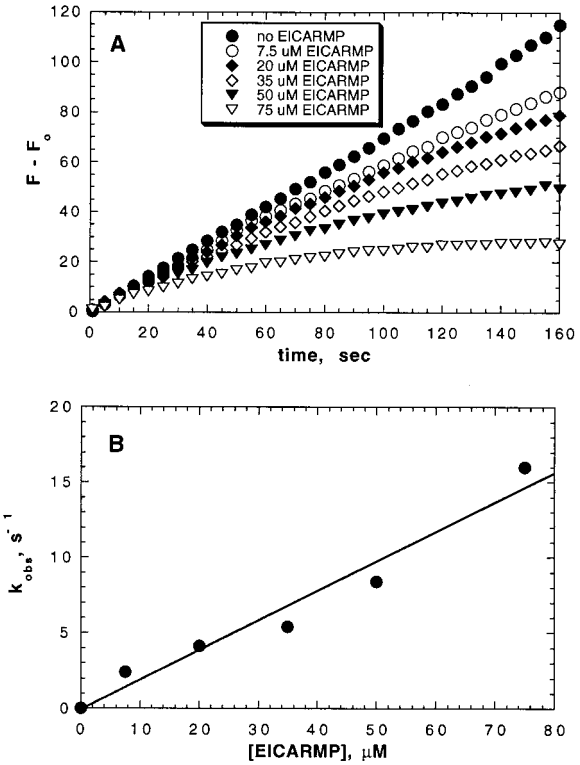

FIGURE 5: EICARMP inactivation of Asp338Ala. (A) Asp338Ala IMPDH (2.8 μM) was incubated with 750 μM IMP and 8 mM NAD^+ in 50 mM Tris, pH 8.0, 100 mM KCl, 3 mM EDTA, 1 mM DTT, and varying concentrations of EICARMP: no EICARMP, closed circles; 7.5 μM, open circles; 20 μM, closed diamonds; 35 μM, open diamonds; 50 μM, closed triangles; 75 μM, open triangles. NADH production was monitored for 2 min. Values of k_{obs} are determined from eq 5. (B) Dependence of k_{obs} on [EICARMP].

EICARMP is perturbed by no less than a factor of 5 (as observed in the values of K_i for GMP and XMP), the rate of alkylation must have decreased by no more than a factor of 12.

The kinetics of the 6-Cl-IMP inactivation of wild-type and Asp338Ala IMPDH were measured as described in Materials and Methods (Table 4). In contrast to EICARMP inactivation,

Table 4: Inactivation of Wild-Type and Asp338Ala IMPDH

	EICARMP		6-Cl-IMP	
enzyme	k_{on} (M^{-1} s^{-1})	k_{on} (M^{-1} s^{-1})	k_{inact} (min^{-1})	K_i (μM)
wild-type	2.3×10^{4a}	150	0.015	97
Asp338Ala	380	27	0.052	1900

[a] Value from ref *13*.

the mutation decreased k_{on} by only 6-fold. Also unlike EICARMP inactivation, the values of k_{inact} and K_i for the inactivation of wild-type and Asp338Ala IMPDH by could also be determined. The value of k_{inact} is in agreement with the value previously reported for the *E. coli* enzyme [$k_{inact} = 0.01$ s^{-1} (*28*)] and similar to that reported for human type 2 IMPDH [$k_{inact} = 0.0035$ min^{-1} (*26*)]. The Asp338 → Ala mutation *increases* the value of k_{inact} by 3-fold. The value of K_i increases by 19-fold. Therefore the substitution of Asp338 decreases the affinity of the inhibitor, as previously observed with XMP and GMP, but does not decrease the reactivity of the active site Cys.

Reaction with 2-Cl-IMP. IMPDH catalyzes the hydrolysis of 2-Cl-IMP to XMP (Figure 4C) (*15*). This reaction is presumed to mimic the normal catalytic mechanism: attack of Cys307 at the 2-position of IMP, expulsion of Cl^- to produce E-XMP*, and subsequent hydrolysis of E-XMP*. Therefore, this reaction monitors both the nucleophilicity of the active site Cys residue and the hydrolysis of E-XMP*. The Michaelis−Menten parameters for the reaction of wild-type IMPDH are $k_{cat} = 0.32 \pm 0.02$ s^{-1} and $K_m = 44 \pm 10$ μM. The value of k_{cat} is only 3% of the value of k_{cat} for the oxidation of IMP. This observation indicates that the hydrolysis of E-XMP* cannot be rate-limiting in the 2-Cl-IMP reaction since the hydrolysis of E-XMP* cannot be less than 13 s^{-1} (the value of k_{cat} for the IMPDH reaction).

The mutation of Asp338 to Ala has a relatively minor effect on the 2-Cl-IMP reaction. The value of k_{cat} decreases by a factor of 8 to 0.040 ± 0.008 s^{-1}, while the value of K_m increases by a factor of 14 to 620 μM. The value of k_{cat} in the 2-Cl-IMP reaction places a lower limit of 0.04 s^{-1} on the hydrolysis of E-XMP* in the reaction of Asp338Ala. This limit is consistent with the lower limit of ≥ 0.1 s^{-1} imposed by the observation that hydride transfer is rate-limiting in oxidation of IMP (hydrolysis of E-XMP* must be greater than $5 \times k_{cat}$).

Construction, Expression, and Characterization of Asp338-Glu and Asp338Asn IMPDHs. Two mutant enzymes, Asp338Glu and Asp338Asn, were constructed to further probe the role of Asp338 in the IMPDH reaction. Asp338Glu is at least 20-fold less active than Asp338Ala as estimated by k_{cat}/K_mK_m (≤ 400 M^{-2} s^{-1}). Unfortunately, the activity of this mutant enzyme was too low to permit the kinetic parameters to be determined with confidence. While significant activity was observed in the Asp338Asn sample, this activity appeared to result from the deamidation of Asn338, which generates wild-type enzyme. Asn338 is found in an Asn−Gly−Gly sequence, which is prone to deamidation (*29*). Unfortunately, the role of Asp338 could not be further investigated using either Asp33Glu or Asp338Asn.

DISCUSSION

The Kinetic Mechanism of E. coli IMPDH. *E. coli* IMPDH is the fastest IMPDH characterized to date, with k_{cat} approximately 30-times greater than that of human IMPDH type 2. A burst of NADH production is observed when the reaction is monitored by absorbance. This burst is linearly dependent on NAD^+ concentration, which suggests that the rate of hydride transfer exceeds 200 s^{-1}. Hydride transfer is followed by a slow step (see below) and therefore must be at equilibrium. Since the amplitude of the burst phase is 0.5 NADH/active site, the equilibrium constant for this step is 1, and the forward and reverse rate constants must be equal and ≥ 100 s^{-1}.

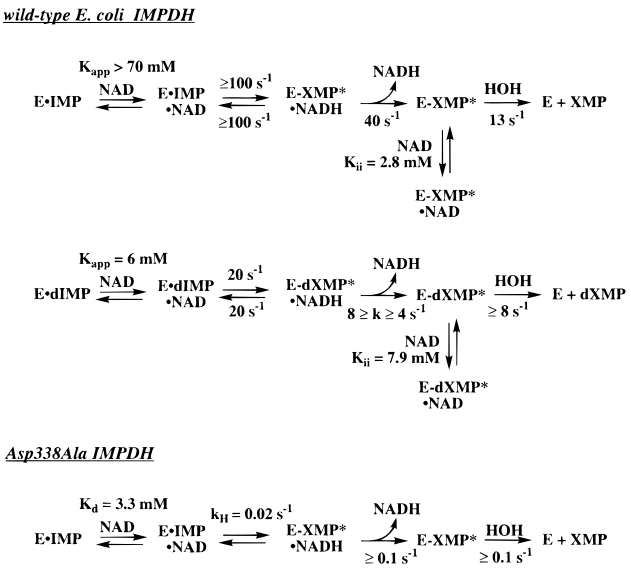

FIGURE 6: Proposed mechanisms for wild-type and Asp338Ala IMPDHs.

A burst is also observed when the reaction is monitored by fluorescence. However, the maximum k_{fluor} is only 40 s^{-1}. We believe that this fluorescence change monitors the release of NADH from the enzyme. Similar conclusions have been made for *T. foetus* and human IMPDH type 2 [(*18*); Digits, J., Wang, W., and Hedstrom, L., unpublished experiments]. Since the value of k_{cat} (13 s^{-1}) is less than 40 s^{-1}, another slow step remains. We have assigned 13 s^{-1} to the rate constant for E-XMP* hydrolysis, again by analogy to the kinetic mechanism for *T. foetus* and human type 2 enzymes (*12*, *18*). A scheme describing the kinetic mechanism of the *E. coli* IMPDH reaction is shown in Figure 6. Interestingly, the rate constants for hydride transfer, NADH release, and E-XMP* hydrolysis are at least 4-fold greater than in the case of *T. foetus* IMPDH. Thus, the higher value of k_{cat} of *E. coli* IMPDH does not derive from the acceleration of a single step but rather from an acceleration of all of the steps.

Kinetics of the dIMP Reaction. Crystal structures indicate that the 2′-OH of IMP may be involved in two hydrogen bonding networks, the first linking Asp338 to N3 of IMP via two water molecules and the second linking Asp338 to the nicotinamide of NAD^+ (Figure 2) (*7*, *9*). The first network could function to activate water for hydrolysis of E-XMP*, while the second network could be important for hydride transfer. We investigated the reaction with dIMP to probe the importance of these networks in the IMPDH reaction. The steady-state kinetic parameters for the dIMP reaction are very similar to the IMP reaction (Table 2). However, the pre-steady-state reaction displays two differences. First,

the rate constant for the absorbance burst phase is lower than that observed in the IMP reaction ($k_{burst} = 40\ s^{-1}$). Second, the rate constant for the fluorescence burst is the same as that measured by absorbance. Therefore, the absorbance and fluorescence measurements monitor the same step. The amplitude of the burst phase is 0.5 NADH/active site, as observed in the IMP reaction. Assuming that the hydride transfer step is at equilibrium as in the IMP reaction, then NADH release is less than 8 s^{-1} ($0.2 \times 40\ s^{-1}$) but greater than 4 s^{-1} (k_{cat}). These conditions also impose a lower limit of 8 s^{-1} on the hydrolysis of E-XMP*. This kinetic mechanism is presented in Figure 6. Thus, the loss of the 2′-OH group of IMP decreases hydride transfer by at least 5-fold while decreasing the hydrolysis of E-XMP* by less than 2-fold. These results suggest that the hydrogen bonding networks involving the 2′-OH, and probably Asp338, serve to accelerate hydride transfer.

The Kinetic Mechanism of Asp338Ala IMPDH. The mutation of Asp338 decreases k_{cat} by 650-fold. Isotope effects and pre-steady state measurements indicate that hydride transfer is completely rate-limiting under these conditions. Therefore, the rate constant for hydride transfer is decreased by at least 5×10^3-fold. Although inhibitor analysis suggests that the mutation has not decreased the reactivity of the active site Cys, we are only able to assign a lower limit to the rate constant for hydrolysis of E-XMP*, so that the mutation decreases the hydrolysis of E-XMP* by less than 100-fold (Figure 6). These observations suggest that Asp338 mainly functions in the hydride transfer step and is not required for hydrolysis of E-XMP*. Thus, Asp338 is not the general base that activates water.

ACKNOWLEDGMENT

We thank Rebecca Myers for DNA sequencing.

REFERENCES

1. Weber, G. (1983) *Cancer Res. 43*, 3466−3492.
2. Pankiewicz, K. W. (1997) *Pharmacol. Ther. 76*, 89−100.
3. DeClerq, E. (1993) *Adv. Virus Res. 42*, 1−55.
4. Halloran, P. F. (1996) *Clin. Transplant. 10*, 118−123.
5. Huete-Perez, J. A., Wu, J. C., Whitby, F. G., and Wang, C. C. (1995) *Biochemistry 34*, 13889−13894.
6. Link, J. O., and Straub, K. (1996) *J. Am. Chem. Soc. 118*, 2091−2092.
7. Sintchak, M. D., Fleming, M. A., Futer, O., Raybuck, S. A., Chambers, S. P., Caron, P. R., Murcko, M., and Wilson, K. P. (1996) *Cell 85*, 921−930.
8. Zhang, R.-G., Evans, G., Rotella, F. J., Westbrook, E. M., Beno, D., Huberman, E., Joachimiak, A., and Collart, F. R. (1999) *Biochemistry 38*, 4691−4700.
9. Colby, T. D., Vanderveen, K., Strickler, M. D., Markham, G. D., and Goldstein, B. M. (1999) *Proc. Natl. Acad. Sci. U.S.A. 96*, 3531−3536.
10. Whitby, F. G., Luecke, H., Kuhn, P., Somoza, J. R., Huete-Perez, J. A., Philips, J. D., Hill, C. P., Fletterick, R. J., and Wang, C. C. (1997) *Biochemistry 36*, 10666−10674.
11. Kerr, K. M., and Hedstrom, L. (1997) *Biochemistry 36*, 13365−13373.
12. Wang, W., and Hedstrom, L. (1997) *Biochemistry 36*, 8479−8483.
13. Wang, W., Papov, V. V., Minakawa, N., Matsuda, A., Biemann, K., and Hedstrom, L. (1996) *Biochemistry 35*, 95−101.
14. Zhou, X., Cahoon, M., Rosa, P., and Hedstrom, L. (1997) *J. Biol. Chem. 272*, 21977−21981.
15. Antonino, L. C., and Wu, J. C. (1994) *Biochemistry 33*, 1753−1759.
16. Markham, G. D., Bock, C. L., and Schalk-Hihi, C. (1999) *Biochemistry 38*, 4433−4440.
17. Hupe, D., Azzolina, B., and Behrens, N. (1986) *J. Biol. Chem. 261*, 8363−8369.
18. Digits, J. A., and Hedstrom, L. (1999) *Biochemistry 38*, 2295−2306.
19. Wu, J. C., Carr, S. F., Antonino, L. C., Papp, E., and Pease, J. H. (1995) *FASEB J. 9*, A1337.
20. Xiang, B., and Markham, G. D. (1997) *Arch. Biochem. Biophys. 348*, 378−382.
21. Cook, P. F. (1991) *Enzyme Mechanism from Isotope Effects*, CRC Press, Boca Raton, FL.
22. Holmes, E., Pehlke, D., and Kelley, W. (1974) *Biochim. Biophys. Acta 364*, 209−217.
23. Carr, S. F., Papp, E., Wu, J. C., and Natsumeda, Y. (1993) *J. Biol. Chem. 268*, 27286−27290.
24. Kerr, K. M., Cahoon, M. C., Bosco, D. A., and Hedstrom, L. (2000) *Arch. Biochem. Biophys. 375*, 131−137.
25. Miller, R., and Adamczyk, D. (1976) *Biochem. Pharm. 25*, 883−888.
26. Antonino, L. C., Straub, K., and Wu, J. C. (1994) *Biochemistry 33*, 1760−1765.
27. Brox, L., and Hampton, A. (1968) *Biochemistry 7*, 2589−2596.
28. Gilbert, H., and Drabble, W. (1980) *Biochem. J. 191*, 533−541.
29. Wright, H. T. (1991) *Protein Eng. 4*, 283−294.
30. Digits, J. A., and Hedstrom, L. (1999) *Biochemistry 38*, 15388−15397.

BI0005409